Journal of Information & Optimization Sciences
ISSN 0252-2667 (Print), ISSN 2169-0103 (Online)
DOI : 10.47974/JIOS-1944

Numerical solution of nonlinear equations of traffic flow density using filter methods with middle-grid point

Seyed Esmaeil Sadat Najafi [§]
Department of Mathematics
Science and Research Branch
Islamic Azad University
Tehran 1477893855
Iran

Tofigh Allahviranloo [†]
Department of Mathematics
Science and Research Branch
Islamic Azad University
Tehran 1477893855
Iran

and

Faculty of Engineering and Natural Sciences
Istinye University
Istanbul 34396
Turkey

Saeid Abbasbandy *
Department of Applied Mathematics
Faculty of Science
Imam Khomeini International University
Qazvin 3414916818
Iran

[§] *E-mail:* seyedesmaeilsadatnajafi@gmail.com
[†] *E-mail:* tofigh.allahviranloo@eng.bau.edu.tr; allahviranloo@gmail.com
* *E-mail:* abbasbandy@sci.ikiu.ac.ir; (Corresponding Author) abbasbandy@yahoo.com

Mohsen Rostamy Malkhalifeh ‡
Department of Mathematics
Science and Research Branch
Islamic Azad University
Tehran 1477893855
Iran

Abstract

This study addresses the significant challenge of accurately simulating traffic flow in heavily congested urban areas through microscopic traffic models. These models employ differential equations to simulate the behavior of individual vehicles, providing valuable insights into traffic patterns and congestion levels. However, conventional numerical techniques, such as the spectral method, often fall short of accurately capturing traffic dynamics, resulting in the introduction of shocks that cause substantial inaccuracies. To overcome this problem, we propose a novel method that incorporates a Discrete Singular Convolution (DSC) filter. This innovative approach effectively manages and reduces shocks during numerical simulations by adaptively combining discrete convolution filters, thus achieving higher accuracy and computational efficiency. Our method significantly minimizes errors in comparison to traditional techniques. We validate our proposed method by applying it For the Lighthill–Whitham–Richards traffic flow model through a series of numerical experiments. The results demonstrate the superior performance of our approach over traditional schemes, such as Lax and Friedrichs. We compare our findings with the analytical solutions of the relevant equations, showcasing the potential of our method to enhance the accuracy of traffic flow modeling. This improvement has promising implications for traffic management and urban planning.

Subject Classification (2020): *65M30, 35L03, 35L20.*

Keywords: *Spectral methods, Moving mesh method, Traffic flow, Middle-grid point, Central-upwind schemes method.*

1. Introduction

The surge in vehicle numbers has led to severe traffic congestion in recent years. Extensive research underscores the crucial link between transportation and tourism, highlighting the need for efficient transport systems within the tourism sector. Effective traffic management is vital to reduce congestion, and this can be achieved by modeling traffic flow using both microscopic and macroscopic approaches. While microscopic models focus on the behavior of individual vehicles, such as their positions and speeds, macroscopic models consider traffic as a continuous flow, described by overall traffic velocity. This study emphasizes macroscopic traffic flow models.

Many analytical and numerical techniques have been designed to address the nonlinear partial differential equations (NPDEs) that characterize various

‡ *E-mail:* **mohsenrostamy@yahoo.com**

flow phenomena, particularly in nonlinear hyperbolic conservation systems [13, 21, 24, 26]. Although analytical solutions to these equations are often complex, numerical methods provide significant insights into the underlying physical processes. Traffic flow models, which are central to the theory of hyperbolic conservation laws, have been extensively researched and refined to enhance traffic management and forecasting [19].

This paper focuses on the macroscopic, non-conservative Lighthill–Whitham–Richards (LWR) traffic flow model [14, 17], which is grounded in the principles of vehicle conservation on roadways. The LWR model is particularly valued for large-scale simulations due to its simplicity and minimal parameter requirements.

Moreover, advanced techniques from fields such as heat transfer and computational fluid dynamics have been adapted to traffic flow modeling [13,16, 26]. These methods improve the precision of traffic flow models by integrating sophisticated computational techniques from other disciplines [1,10,18,20, 22].

Direct application of spectral methods can lead to solution deviations, often appearing as shocks [4]. Spectral methods typically produce minimal numerical dispersion when approximating derivatives. However, in cases of discontinuities, derivative computations can result in numerous fluctuations and shocks. To address these Gibbs phenomena, we use a non-oscillating weighted approach. This method optimizes viscosity to minimize errors. By incorporating both high-pass and low-pass filters, it effectively handles discontinuities and controls shocks [5, 15, 23, 32]. The use of low-pass filters in this approach helps manage a broad range of waves, thereby improving accuracy in spectral applications [2, 8, 9, 25, 30, 31].

In the realm of spectral methods, various filters are commonly employed, including the Lanczos filter, raised cosine filter, sharp raised cosine filter, and cutoff filter, as listed by Hussain et al. [7]. Additionally, the field of p-filters [29] provides alternative and more effective filter types. These filters are essential components of central schemes that incorporate protection rules on space-time control volumes. Thus, central schemes can be extended to problems involving wave solutions. One of the earliest central schemes is the first-order Lax and Friedrichs scheme [3], widely used for time-dependent PDEs, although with relatively low resolution.

In summary, this work introduces a novel strategy for managing shock waves and fluctuations for modeling traffic flow through integrating spectral methods and PDE filters. This approach not only improves the numerical solution's accuracy and convergence speed but also has practical applications in urban planning and traffic management. The effectiveness of this method depends on the optimal selection of filters and a thorough understanding of the problem's specific characteristics.

2. Theory and Algorithm

Following the methodology established in [27], we assume equidistant points defined as:

$$t_n = t_0 + n\Delta t,\ x_j = x_0 + j\Delta x,\ j = 1, \dots, N. \quad (1)$$

We use the DSC filter to compute $\varrho^{(1)}(x)$ as follows. As described in [27], The following convolution provides the theoretical definition of a filter:

$$\Gamma(x) = (\Theta * \tau)(x) = \int_{-\infty}^{\infty} \Theta(x-t)\tau(t)dt, \quad (2)$$

where $\Theta(.)$ and $\tau(.)$ are described in [27]. Various types of kernel functions exist [27]. In this work, we utilize Delta kernels, which are expressed as follows:

$$\Theta(x) = \varsigma_{\alpha,\beta}^{(s)}(x), s = 0,1,2, \dots, \quad (3)$$

here, s represents the degree of the derivative, and the kernel function utilized is derived from the Shannon function:

$$\varsigma_{\alpha,\beta}(x - x_k) = \frac{\sin(\frac{\pi(x-x_k)}{\beta})}{\frac{\pi(x-x_k)}{\beta}} e^{-\frac{(x-x_k)^2}{2\alpha^2}}, \quad (4)$$

the kernel function is regulated by the parameters α and β. Following [27], the interpolation for a function $\rho(x)$ at points ${x_k}_{k=-\mu}^{\mu}$ is expressed as:

$$\varrho^{(s)}(x) \approx \sum_{k=-\mu}^{\mu} \varsigma_{\alpha,\beta}^{(s)}(x - x_k)\rho(x_k), s = 0,1,2, \dots. \quad (5)$$

For $s = 0$, the expressions for $\varsigma_{\alpha,\beta}^{(s)}$ are:

$$\varsigma_{\alpha,\beta}(x) = \begin{cases} \frac{\sin(\frac{\pi}{\beta}(x))}{\frac{\pi}{\beta}(x)} e^{-(x)^2/(2\alpha^2)}, & x = 0, \\ 1, & x \neq 0. \end{cases} \quad (6)$$

For $s = 1$, they are:

$$\varsigma_{\alpha,\beta}^{(1)}(x) = \begin{cases} \frac{\cos\left(\frac{\pi x}{\beta}\right) e^{\frac{-x^2}{2\alpha^2}}}{x} - \frac{sin\left(\frac{\pi x}{\beta}\right) e^{\frac{-x^2}{2\alpha^2}}}{\pi x^2 \beta} - \frac{sin\left(\frac{\pi x}{\beta}\right) e^{\frac{-x^2}{2\alpha^2}}}{\frac{\pi \alpha^2}{\beta}}, & x \neq 0, \\ 0, & x = 0. \end{cases} \quad (7)$$

This study builds upon [27] by employing a different strategyâ€"computing the interpolator function of the filter at intermediate points, denoted as $x_{j+1/2}$, rather than at the traditional x_j points. This modification enhances accuracy and flexibility in derivative calculations, leading to increased sensitivity to shocks and improved solution quality:

$$\varrho^{(s)}(x) \approx \sum_{k=-\mu}^{\mu} \varsigma_{\alpha,\beta}^{(s)}(x - x_{k+1/2})\rho(x_k), s = 0,1,2, \dots, \quad (8)$$

here, $r = \alpha/\beta$ serves as a coefficient that regulates the filter's effectiveness in mitigating shocks. By applying Eq. (7) along with $\varrho^{(1)}(x)$, we develop a method for solving differential equations, extending the results from [27]. As previously noted in [27], smooth solutions are achieved, but discontinuities can lead to oscillations. To mitigate these, slope constraints are applied. The concept was studied by Leer [12].

Any total variation reduction method ensures uniformity. If a discontinuous wave is processed using an exponential total variation reduction method, the discontinuity may persist in subsequent time steps, but oscillations will be eliminated. A suitable approach for computing the slope s_j^n while maintaining the (TVD) property is the Minmod slope function:

$$s_j^n = Minmod\left(\kappa \frac{\bar{\varrho}_j^n - \bar{\varrho}_{j-1}^n}{\Delta x}, \rho^{(1)}(x), \kappa \frac{\bar{\varrho}_{j+1}^n - \bar{\varrho}_j^n}{\Delta x}\right), \ \kappa = 1 \ or \ 2, \tag{9}$$

and

$$Minmod(\zeta_1, \zeta_2, \dots) = \begin{cases} \min\limits_j\{\zeta_j\}, & \zeta_j > 0, \\ \max\limits_j\{\zeta_j\}, & \zeta_j < 0, \\ 0, & o.w., \end{cases} \tag{10}$$

where κ can be chosen as either 1 or 2. In our examples, we set $\kappa = 1$, which resulted in lower residual errors.

The (TVD) concept was introduced in [6]. The term $\varrho^{(1)}(x)$ represents the first derivative obtained using the DSC filter method, as discussed in [27]. We utilize CU schemes [11] as follows:

$$\begin{aligned} \varrho_{j+1}^n \ &= \frac{\bar{\varrho}_j^n + \bar{\varrho}_{j+1}^n}{2} + \frac{1}{8}(\Delta x)\left(s_j^n - s_{j+1}^n\right) \\ &- \frac{\Delta t}{\Delta x}\left(\Psi\left(\bar{\varrho}_{j+1}^n + \frac{1}{2}(\Delta t)s_{j+1}^n\right) - \Psi\left(\bar{\varrho}_j^n + \frac{1}{2}(\Delta t)s_j^n\right)\right). \end{aligned} \tag{11}$$

3. Apply in moving mesh method

Following the methodology outlined in [27], we consider the following equation,

$$\begin{cases} \frac{\partial \varrho}{\partial t} + \frac{\partial(\Psi(\varrho))}{\partial x} = 0, \\ \varrho(x,0) = \varrho_0(x), \\ \varrho(0,t) = 0. \end{cases} \tag{12}$$

This relationship is explained in detail in [27].

$$v = \left(1 - \frac{\varrho}{\varrho_{max}}\right) v_{max}. \tag{13}$$

This formulation aligns with the approach described in [27], where similar conservation principles are applied to traffic flow modeling.

4. Method convergence

To analyze the stability and convergence of the method, we utilize the Courant-Friedrichs-Lewy criterion, as described in [27]. This condition is expressed as:

$$|\Psi_x(\varrho)\frac{\Delta t}{\Delta x}| \leq 1, \tag{14}$$

for conversion law equation,

$$\varrho_t + \Psi_x(\varrho) = 0. \tag{15}$$

Following the methodology introduced in [27], we utilize the Courant number, which is constrained by c, to enhance accuracy. This leads to the condition,

$$\Delta t \leq c.\min_{j} \frac{\Delta x}{|\Psi_x(\varrho_j^n)|},\ j = 1, \dots, N,\ n = 1, \dots, N_t, 0 < c < 1, \tag{16}$$

where ϱ_j^n represents the numerical value of ρ at spatial point x_j and time t_n. As shown in [27], satisfying this condition ensures the convergence of the numerical scheme. In this method $\Psi_x(\rho_j^n) = s_j^n$ then if find a upper limit for s_j^n we can know this method satisfy CFL condition. Using this procedure, as derived in [27], $s_j^n = \frac{\overline{\varrho}_j^n - \overline{\varrho}_{j-1}^n}{\Delta x}$, $s_j^n = \frac{\overline{\varrho}_{j+1}^n - \overline{\varrho}_j^n}{\Delta x}$ or $s_j^n = \varrho^{(1)}(x_j)$ where ϱ represents density,

$$\left|\frac{\overline{\varrho}_j^n - \overline{\varrho}_{j-1}^n}{\Delta x}\right| \leq \frac{1}{\Delta x} \text{ and } \left|\frac{\overline{\varrho}_{j+1}^n - \overline{\varrho}_j^n}{\Delta x}\right| \leq \frac{1}{\Delta x}, \tag{17}$$

then,

$$\Delta t \leq c.\min_{j} \frac{\Delta x}{|s_j^n|} \leq \frac{\Delta x}{\frac{1}{\Delta x}} \Rightarrow \Delta t \leq (\Delta x)^2 \Rightarrow \frac{\Delta t}{(\Delta x)^2} \leq 1. \tag{18}$$

Thus, the CFL condition is satisfied if $\frac{\Delta t}{(\Delta x)^2} \leq 1$, consistent with prior results in [27]. Next, we analyze the case where $s_j^n = \varrho^{(1)}(x_j)$,

$$\begin{aligned}\Psi_x(\varrho_j^n) &= (\textstyle\sum_{k\neq j, k=j-\frac{\mu}{2}}^{j+\frac{\mu}{2}} \frac{\partial \varsigma_{\beta,\alpha}(x - x_{k+1/2})}{\partial x}(x_j)\varrho(x_k, t))(2\varrho(x_j, t) - 1)\\ &= (\textstyle\sum_{k\neq j, k=j-\frac{\mu}{2}}^{j+\frac{\mu}{2}} \varsigma_{\alpha,\beta}^{(1)}(x_j)\varrho(x_k, t))(2\varrho(x_j, t) - 1).\end{aligned} \tag{19}$$

Since, based on the density function of u, the following holds [11]. As discussed in [27], the density function u satisfies the following property:

$$0 \leq \varrho_j^n \leq 1 \Rightarrow \max_{1\leq j\leq N} |2\varrho_j^n - 1| \leq 1, \tag{20}$$

which leads to,

$$\max_{j} |\Psi_x(\varrho_j^n)| \leq \max_{j} |\textstyle\sum_{k\neq j, k=j-\frac{\mu}{2}}^{j+\frac{\mu}{2}} \frac{\partial \varsigma_{\beta,\alpha}^{(1)}(x - x_{k+1/2})}{\partial x}(x_j)\varrho(x_k, t)|, \tag{21}$$

$$\leq \textstyle\sum_{k\neq j, k=j-\frac{\mu}{2}}^{j+\frac{\mu}{2}} \max_{j} |\frac{\partial \varsigma_{\beta,\alpha}^{(1)}(x - x_{k+1/2})}{\partial x}(x_j)\varrho(x_k, t)| \tag{22}$$

$$= \textstyle\sum_{k\neq j, k=j-\frac{\mu}{2}}^{j+\frac{\mu}{2}} \max_{j} |\frac{\cos(\frac{\pi x}{\beta}) e^{\frac{-x^2}{2\alpha^2}}}{x} - \frac{\sin(\frac{\pi x}{\beta}) e^{\frac{-x^2}{2\alpha^2}}}{\pi x^2 \beta} - \frac{\sin(\frac{\pi x}{\beta}) e^{\frac{-x^2}{2\alpha^2}}}{\frac{\pi\alpha^2}{\beta}}|.|\varrho(x_k, t)|. \tag{23}$$

Since $0 \leq \varrho \leq 1$, then

$$\max_{j} |\Psi_x(\varrho_j^n)| \leq \textstyle\sum_{k\neq j, k=j-\frac{\mu}{2}}^{j+\frac{\mu}{2}} \max_{j} |\frac{\cos(\frac{\pi(x_j - x_k)}{\beta})\, e^{\frac{-(x_j - x_k)^2}{2\alpha^2}}}{(x_j - x_k)} - \frac{\sin(\frac{\pi(x_j - x_k)}{\beta}) e^{\frac{-(x_j - x_k)^2}{2\alpha^2}}}{\pi(x_j - x_k)^2\beta}$$

$$- \frac{\sin(\frac{\pi(x_j - x_k)}{\beta}) e^{\frac{-(x_j - x_k)^2}{2\alpha^2}}}{\frac{\pi\alpha^2}{\beta}}|, \tag{24}$$

in this method $\beta = \Delta x$, then

$$\max_j|\Psi_x(\varrho_j^n)| \leq \sum_{k\neq j,k=j-\frac{\mu}{2}}^{j+\frac{\mu}{2}} \frac{\max_j|e^{\frac{-(x_j-x_k)^2}{2\alpha^2}}|}{\Delta x} + \frac{\max_j|e^{\frac{-(x_j-x_k)^2}{2\alpha^2}}|}{\pi(\Delta x)^3} + \frac{\max_j|e^{\frac{-(x_j-x_k)^2}{2\alpha^2}}|}{\frac{\pi\alpha^2}{\Delta x}}. \quad (25)$$

Since $e^{\frac{-(x_j-x_k)^2}{2\alpha^2}} \leq 1$, then

$$\begin{aligned}\max_j|\Psi_x(\varrho_j^n)| &\leq \sum_{k\neq j,k=j-\frac{\mu}{2}}^{j+\frac{\mu}{2}} (\Delta x)^{-1} + (\pi(\Delta x)^3)^{-1} + (\frac{\pi\alpha^2}{\Delta x})^{-1} \\ &= (\mu-1)((\Delta x)^{-1} + (\pi(\Delta x)^3)^{-1} + (\frac{\pi\alpha^2}{\Delta x})^{-1}),\end{aligned} \quad (26)$$

and hence

$$\max_j|\Psi_x(\varrho_j^n)| \leq (\mu-1)((\Delta x)^{-1} + (\pi(\Delta x)^3)^{-1} + \left(\frac{\pi\alpha^2}{\Delta x}\right)^{-1}\Big) \text{ and } \frac{\Delta t}{(\Delta x)^2} <= 1. \quad (27)$$

Since the expression on the right is explicitly computable, the method is proven to be convergent, reinforcing the findings in [27]. However, in this study, we extend the analysis by incorporating middle-grid point interpolation, improving numerical accuracy in handling shock formations and stability constraints.

5. Computational results

Sample Case 1.

We examine he LWR model for traffic flow presented in [27] as follows:

$$\begin{cases}\frac{\partial\varrho}{\partial t} + \frac{\partial(\Psi(\varrho))}{\partial x} = 0, \\ \varrho(0,t) = 0, \\ \varrho(x,0) = \begin{pmatrix}1, x \leq 0, \\ 0, x > 0.\end{pmatrix}\end{cases} \quad (28)$$

We suppose that $\Psi(\varrho) = \rho v$, $\varrho_{max} = 1$, $v_{max} = 1$, $v = v_{max}(1 - \varrho/\varrho_{max})$ [27], where the solution is explicitly given by,

$$\rho(x,t) = \begin{cases}1 \ , \ \frac{x}{t} \leq \Psi'(0) \ , \\ \frac{1}{2} \ \varrho_{max}(1 - \frac{x}{t \ \rho_{max}}) \ , \ \Psi'(1) \leq \frac{x}{t} < \Psi'(0), \\ 0 \ , \ \frac{x}{t} \geq \Psi'(0).\end{cases} \quad (29)$$

Following the computational setup in [27], we use $\Delta_0 = \frac{L}{N}$, $\mu = 32$, $\alpha = \beta.r$, and apply the technique of filtering based on spectral properties for the obtained result for $t = 1$. Additional parameters include $\Delta t^n = \frac{\Delta x^n}{10}$, $L = 20$, $r = 0.5$, $c = 0.5$ and N is chosen as 500. Fig. 1 displays the graph of the numerical solution to the traffic flow model using the adaptive filter method for density. Fig. 2 compares the current approach with the exact solution, showing improvements in accuracy. The right side of Eq. (27) is 6141. The lowest numerical constraint of the Courant condition, calculated as $c\frac{\Delta x_j}{\min_j F_\rho(\rho_j^n)} =$

$1.24e-01$, aligns with the results in [27]. Table 1 compares the Error method with the Lax and Friedrichs methods. The results indicate that the L_2 error of the proposed approach, relative to the analytical solution, is $5.8321e-03$.

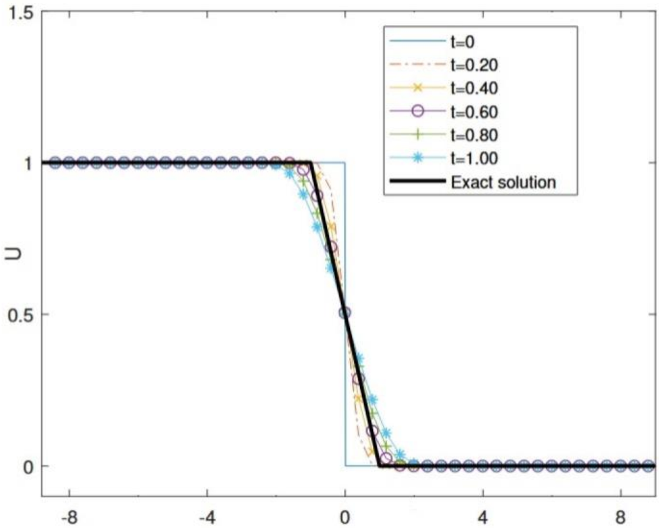

Figure 1
Traffic flow model solution using the current approach: density as a function of location at $t = 1$ in Sample Case 1.

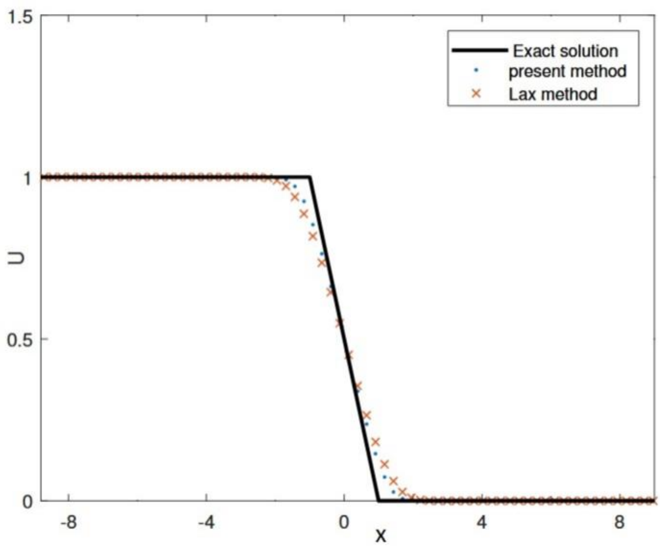

Figure 2
Compare current approach with lax and exact solution in Sample Case 1.

Table 1
Evaluation errors for the current approach and the Lax scheme in an Sample Case 1

current approach L2 error	Lax scheme L_2 error	t times
6.2443e-03	3.8623e-02	0.2
3.6165e-03	2.4367e-01	0.4
3.7278e-02	2.2642e-01	0.6
3.2345e-02	1.1686e-01	0.8
3.0441e-02	2.1935e-01	1

Sample Case 2.

For the second case, we analyze a relaxation model for traffic flow [28], following the framework established in [27], which has been adjusted based on the principle of forward-looking. The governing equation is given by:

$$\begin{cases} \frac{\partial \varrho}{\partial t} + \frac{e^{-\varrho}\, \partial(\rho(1-\rho))}{\partial x} = \alpha(\varrho_{eq} - \varrho), \\ \varrho(x,0) = \begin{pmatrix} 1, & 4 < x < 6, \\ 0, & o.w., \end{pmatrix} \\ \varrho(0,t) = 0. \end{cases} \tag{30}$$

Consistent with the approach in [27], we use $\mu = 32$, $\sigma = \beta.r$, and apply the technique of filtering based on spectral properties. The solution is obtained at $t = 25$, with parameters $\Delta t = \frac{\Delta x}{10}$, $L = 65$, $r = 0.5$, $c = 0.5$, $\alpha = 0.5$, and $\rho_{eq} = 0.8$ and N is chosen as 500. Fig. 3 presents the solution of the current approach for density, while Fig. 4 illustrates the density evolution and its accumulation over time. In this case, the expression on the right side of Eq. (27) is 4921, consistent with the findings in [27]. In Table 2, we evaluate the L_2 norm of the error of the current approach in comparison with Lax and Friedrichs. The lowest numerical constraint of the Courant condition is expressed as $\frac{\Delta x c}{\min\limits_{j} \Psi_\rho(\rho_j^n)} = 1.12e-01$, demonstrating the stability of the approach as discussed in [27].

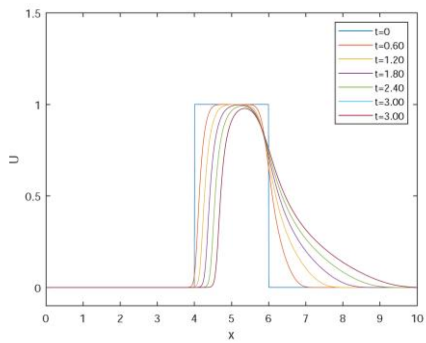

Figure 3
Traffic flow model solution using the current approach: density as a function of location at $t = 3$ in Sample Case 2.

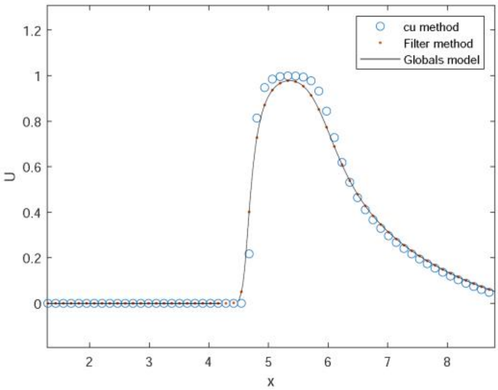

Figure 4
Density and accumulation of density versus location over time in Sample Case 2.

Table 2
$L2$ error for Sample Case 2.

Current approach	CU method	t
4.7543e-03	6.2854e-03	0.6
4.1923e-03	5.8293e-03	1.2
4.0118e-03	5.6753e-03	1.8
3.9194e-03	5.6001e-03	2.4
3.8503e-03	5.5653e-03	3.0

Sample Case 3.

For the third case, we consider a relaxation model for traffic flow that has been adjusted based on the forward-looking law, as follows [11].

$$\begin{cases} \frac{\partial \varrho}{\partial t} + V_m \frac{e^{-\varrho}\, \partial(\varrho(1-\rho))}{\partial x} = \alpha(\varrho_{eq} - \varrho), \\ \varrho(0,t) = 0, \\ \varrho(x,0) = \begin{pmatrix} 1, & 4 < x < 6, \\ 0, & o.w. \end{pmatrix} \end{cases} \tag{31}$$

Following the methodology outlined in [27], we employ $\mu = 32$, $\beta = \frac{L}{N}$, $\sigma = \beta . r$, and the technique of filtering based on spectral properties. the obtained result for $t = 1$ is computed with $Vm = 2$, $\Delta t = \frac{\Delta x}{10}$, $L = 10$, $r = 0.5$, $c = 0.5$, $\alpha = 0.5$, and $\varrho_{eq} = 0.8$ and N is chosen as 500. Fig. 5 presents the solution using the current approach and compares it with the CU method, as referenced in [27]. Additionally, Fig. 6 illustrates the results obtained using both the CU scheme and [11].

In this example, the expression Eq. (27) is 9835. Table 3 provides a comparative analysis of the $L2$ error between the current approach and the Lax and Friedrichs method. The lowest numerical constraint of the the Courant condition is expressed as $\frac{\Delta xc}{\min_j \Psi_\rho(\rho_j^n)} = 1.51e - 02$, consistent with the findings in [27].

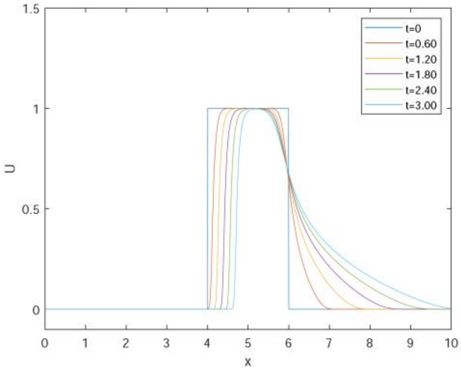

Figure 5
Traffic flow model solution using the current approach: density as a function of location at $t = 3$ in Sample Case 3.

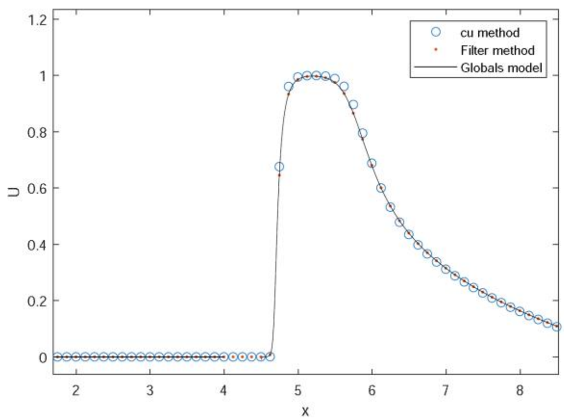

Figure 6
In Sample Case 3, the density distributions computed using the proposed method and CU schemes are plotted against location.

Table 3
$L2$ error for Sample Case 3.

Current approach	CU method	t
6.9918e-03	7.0104e-03	0.6
6.6804e-03	6.9968e-03	1.2
6.5868e-03	6.6154e-03	1.8
6.5338e-03	6.5981e-03	2.4
6.5082e-03	6.5432e-03	3

Sample Case 4.

Following the methodology established in [27], we consider the following example,

$$\begin{cases} \frac{\partial \varrho}{\partial t} + \frac{\partial(\varrho(1-\varrho))}{\partial x} = 0, \\ \varrho(x,0) = \frac{1}{4} + 0.7e^{-x^2 10^{-2}}, \\ \varrho(0,t) = 0. \end{cases} \tag{32}$$

Following the methodology in [27], we use $\mu = 32$, $\beta = \frac{L}{N}$, $\sigma = r.\beta$, and the technique of filtering based on spectral properties to obtain the obtained result for $t = 25$, with parameters $\Delta t = \frac{\Delta x}{10}$, $r = 0.5$, $L = 65$, $c = 0.5$ and N is chosen as 500. Fig. 7 displays the graph of numerical solution to the traffic flow model by filter method density, Fig. 8 has been prepared with CLAWPACK software, and Fig. 9 shows the density and accumulation of density over time. Fig. 7 provides the computed approximation, and Fig. 9 illustrates the density and its accumulation over time. In this example, the expression Eq. (26) is 5035. In Table 4, we evaluate the error of the current method in comparison with Lax and Friedrichs, following the approach in [27]. The lowest numerical constraint of the Courant condition is expressed as $\frac{\Delta x c}{\min_j \Psi_\rho(\rho_j^n)} = 1.71e-01$.

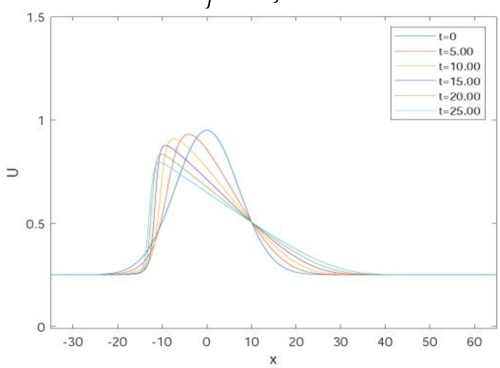

Figure 7
In Sample Case 4, the density distribution at $t = 25$, is shown as a function of location.

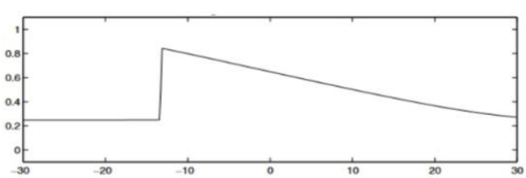

Figure 8
The diagram above has been generated using CLAWPACK software in Sample Case 4.

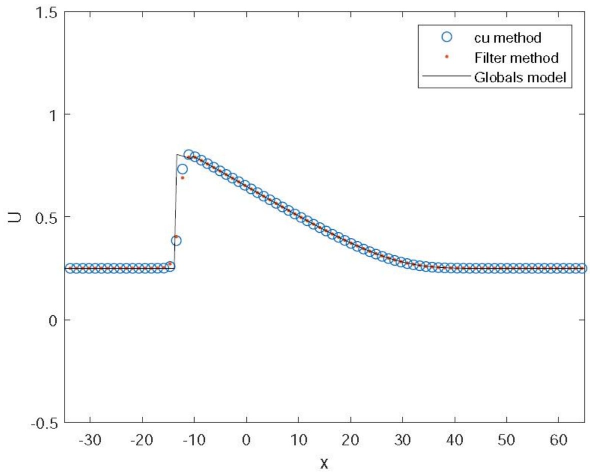

Figure 9
Density and accumulation of density as a function of location over time in Sample Case 4.

Table 4
$L2$ error for Sample Case 4.

Current approach	CU method	t
4.3245e-04	4.3993e-04	0.03
3.9776e-04	4.1659e-04	6.50
3.1828e-04	3.7383e-04	13.00
2.2492e-04	2.9384e-04	19.50
1.5305e-04	2.2291e-04	25.00

Sample Case 5.

For the fiftieth case, particularly Burgers' equation, modified based on the forward-looking law, as shown below,

$$\begin{cases} \frac{\partial \varrho}{\partial t} - \varepsilon \frac{\partial^2(\varrho)}{\partial x^2} + \varrho \frac{\partial(\varrho)}{\partial x} = 0, \\ \varrho(x,0) = \sin(2\pi x) + \frac{1}{2}\sin(\pi x), \\ \varrho(0,t) = 0, \varrho(0,1) = 0. \end{cases} \tag{33}$$

Following the methodology presented in [27], we use $\mu = 32$, $\beta = \frac{L}{N}$, $\sigma = \beta . r$, and the technique of filtering based on spectral properties to obtain the value of the obtained result for $t = 1$, with parameters $\Delta t = \frac{\Delta x}{10}$, $L = 1$, $\varepsilon = 0.0001$, $r = 0.5$, $c = 0.5$ and N is chosen as 500. In Table 5, we evaluate the L_2 norm of error of the current method , following the approach outlined in [27]. Fig. 10 shows the solution is demonstrated using the proposed method.

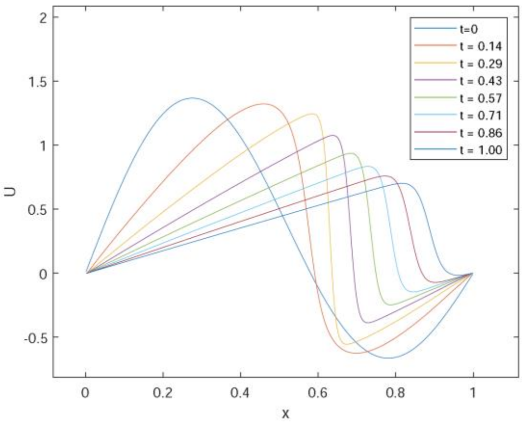

Figure 10
The current approach at $t = 1$ in Sample Case 5.

Table 5
$L2$ error for Sample Case 5.

Current approach	Lax scheme	t
3.3773e-01	1.7843e+01	0.2
3.0569e-01	1.8126e+01	0.4
2.0065e-01	7.8281e+00	0.6
1.4106e-01	3.5409e+00	0.8
1.0555e-01	2.3983e+00	1.0

6. Conclusions

Our approach combines central-upwind schemes and the filter method at middle-grid points, resulting in improved stability for the spectral method over long periods. We have employed the fourth-order Runge-Kutta method in the time domain to implement this method, which is computationally efficient, less complex, and offers greater flexibility compared to non-middle-grid point methods. By adjusting the parameters of this method, we can adapt it to a wide range of equations. We have conducted numerical comparisons with other methods in several cases, and the findings show that our method produces smaller error rates than the other methods presented in the paper. This demonstrates the successful application of our method in modeling traffic flow problems represented by differential equations. Moreover, this method can be easily extended to higher dimensions and applied to more complex problems. Furthermore, our method can be combined with the Fourier pseudo-spectrum for certain modeling scenarios, which further reduces fluctuations. Additionally, techniques such as using filter midpoints can enhance the resolution of the method. Further research can focus on adapting and refining our method to enhance its precision and minimize computational costs. In conclusion, the central-upwind schemes and filter method provide a reliable and efficient approach for modeling traffic flow problems described by differential equations. With its flexibility and ease of use, this method holds promise for a wide range of applications and can be enhanced to achieve higher accuracy while reducing computational demands.

Author Contribution Statement

All authors have participated equally in (a) drafting the article and revising it critically for important intellectual content; and (b) approval of the final version.

Conflict of interest Statement

The authors have no affiliation with any organization with a direct or indirect financial interest in the subject matter discussed in the manuscript.

Acknowledgements

We thank the anonymous reviewers for helpful comments, which lead to definite improvement in the manuscript.

References

[1] A. I. Delis, I. K. Nikolos, and M. Papageorgiou, "High-resolution numerical relaxation approximations to second-order macroscopic traffic flow models," *Transportation Research Part C: Emerging Technologies,* vol. 44, pp. 318–349 (2014).

[2] N. Dong, "Research and application of image enhancement technology in traffic scene of fog and haze," *Journal of Interdisciplinary Mathematics,* vol. 21, no. 5, pp. 1297–1301 (2018).

[3] K. O. Friedrichs, "Symmetric hyperbolic linear differential equations," *Communications on Pure and Applied Mathematics,* vol. 7, no. 2, pp. 345–392 (1954).

[4] D. Gottlieb, "Issues in the application of high order schemes," *Algorithmic Trends in Computational Fluid Dynamics. Springer,* pp. 195–218 (1991).

[5] Y. Gu and G. W. Wei, "Conjugate filter approach for shock capturing," *Communications in Numerical Methods in Engineering,* vol. 19, no. 2, pp. 99–110 (2003).

[6] A. Harten, "High resolution schemes for hyperbolic conservation laws," *Journal of Computational Physics*, vol. 135, no. 2, pp. 260–278 (1997).

[7] M. Y. Hussaini, D. A. Kopriva, M. D. Salas, and T. A. Zang, "Spectral methods for the Euler equations. I-Fourier methods and shock capturing," *AIAA Journal*, vol. 23, no. 1, pp. 64–70 (1985).

[8] M. Kara and A. Seçgin, "Discrete singular convolution method for modelling of waveguide interaction of beam-type structures with impedance boundaries," *Engineering Structures*, vol. 247, p. 113209 (2021).

[9] M. Kara and A. Seçgin, "Discrete singular convolution method for one-dimensional vibration and acoustics problems with impedance boundaries," *Journal of Sound and Vibration*, vol. 446, pp. 22–36 (2019).

[10] A. Kurganov, S. Noelle, and G. Petrova, "Semidiscrete central-upwind schemes for hyperbolic conservation laws and Hamilton–Jacobi equations," *SIAM Journal on Scientific Computing*, vol. 23, no. 3, pp. 707–740 (2001).

[11] A. Kurganov and A. Polizzi, "Non-oscillatory central schemes for traffic flow models with Arrhenius look-ahead dynamics," *Networks and Heterogeneous Media*, vol. 4, no. 3, pp. 431–451 (2009).

[12] B. V. Leer, "Towards the ultimate conservative difference scheme I. The quest of monotonicity," Proceedings of the Third International Conference on Numerical Methods in Fluid Mechanics, H. Cabannes and R. Temam, Eds., vol. 18, Lecture Notes in Physics. Springer, Berlin, Heidelberg, pp. 163–168 (1973).

[13] R. J. LeVeque, Finite Volume Methods for Hyperbolic Problems, vol. 31. Cambridge, U.K.: Cambridge University Press (2002).

[14] M. J. Lighthill and G. B. Whitham, "On kinematic waves II. A theory of traffic flow on long crowded roads," Proceedings of the Royal Society of London. Series A. *Mathematical and Physical Sciences*, vol. 229, no. 1178, pp. 317–345 (1955).

[15] X. Luo and S. Wu, "An improved WENO-Z+ scheme for solving hyperbolic conservation laws," *Journal of Computational Physics*, vol. 445, p. 110608 (2021).

[16] R. M. M. Mattheij, S. W. Rienstra, and J. H. M. Ten Thije Boonkkamp, Partial Differential Equations: Modeling, Analysis, Computation. Philadelphia, PA: SIAM (2005).

[17] K. Mohamed and M. A. E. Abdelrahman, "The modified Rusanov scheme for solving the ultra-relativistic Euler equations," European Journal of Mechanics-B/Fluids, vol. 90, pp. 89–98, 2021.

[18] K. Mohamed, S. Sahmim, and M. A. E. Abdelrahman, "A Predictor–corrector scheme for simulation of two-phase granular flows over a moved bed with a variable topography," European Journal of Mechanics-B/Fluids, vol. 96, pp. 39–50, 2022.

[19] S. Mohammadian, Z. Zheng, M. M. Haque, and A. Bhaskar, "Performance of continuum models for real-world traffic flows: Comprehensive benchmarking," Transportation Research Part B: Methodological, vol. 147, pp. 132–167, 2021.

[20] H. Nessyahu and E. Tadmor, "Non-oscillatory central differencing for hyperbolic conservation laws," Journal of Computational Physics, vol. 87, no. 2, pp. 408–463, 1990.

[21] C. Nwaigwe and S. Mungkasi, "Comparison of different numerical schemes for 1D conservation laws," Journal of Interdisciplinary Mathematics, vol. 24, no. 3, pp. 537–552, 2021.

[22] D. Ngoduy and R. Liu, "Multiclass first-order simulation model to explain non-linear traffic phenomena," Physica A: Statistical Mechanics and its Applications, vol. 385, no. 2, pp. 667–682, 2007.

[23] A. Shi, P.-O. Persson, and M. J. Zahr, "Implicit shock tracking for unsteady flows by the method of lines," Journal of Computational Physics, vol. 454, p. 110906, 2022.

[24] A. Singh, A. Parwaliya, A. Kumar, A. Elsonbaty, and A. A. Elsadany, "Complex dynamics and bifurcations analysis of discrete-time modified Leslie–Gower system," New Mathematics and Natural Computation (NMNC), vol. 20, no. 03, pp. 857–882, 2024.

[25] Y. Sun, Y. C. Zhou, S.-G. Li, and G. W. Wei, "A windowed Fourier pseudospectral method for hyperbolic conservation laws," Journal of Computational Physics, vol. 214, no. 2, pp. 466–490, 2006.

[26] E. F. Toro et al., Riemann Solvers and Numerical Methods for Fluid Dynamics: A Practical Introduction. Berlin, Heidelberg: Springer, 2009.

[27] S. E. S. Najafi, T. Allahviranloo, S. Abbasbandy, and M. R. Malkhalifeh, "Numerical solution of nonlinear equations of traffic flow density using spectral methods by filter," Journal of Applied Mathematics and Computing, vol. 71, no. 1, pp. 743–763, 2025.

[28] M. Treiber and A. Kesting, Traffic Flow Dynamics: Data, Models and Simulation. Berlin, Germany: Springer-Verlag (2013).

[29] H. Vandeven, “Family of spectral filters for discontinuous problems,” *Journal of Scientific Computing*, vol. 6, pp. 159–192 (1991).

[30] D. C. Wan, B. S. V. Patnaik, and G. W. Wei, “Discrete singular convolution–finite subdomain method for the solution of incompressible viscous flows,” *Journal of Computational Physics,* vol. 180, no. 1, pp. 229–255 (2002).

[31] X. Wang and Z. Yuan, “Discrete singular convolution and Taylor series expansion method for free vibration analysis of beams and rectangular plates with free boundaries,” *International Journal of Mechanical Sciences*, vol. 122, pp. 184–191 (2017).

[32] Y. C. Zhou and G. W. Wei, “High resolution conjugate filters for the simulation of flows,” *Journal of Computational Physics*, vol. 189, no. 1, pp. 159–179 (2003).

Received August, 2024